NIH Public Access
Author Manuscript
Mol Pharm. Author manuscript; available in PMC 2013 March 16.

Published in final edited form as:
Mol Pharm. 2011 June 6; 8(3): 709–715. doi:10.1021/mp100272k.

A Covalently Stabilized lipid-polycation-DNA (sLPD) Vector for Antisense Oligonucleotide Delivery

Xiaojuan Yang[†,‡], **Yong Peng**[‖,⊥], **Bo Yu**[‡,§], **Jianhua Yu**[‖], **Chenguang Zhou**[†,‡], **Yicheng Mao**[†,‡], **L. James Lee**[‡,§], and **Robert J. Lee**[†,‡,‖,*]

[†]Division of Pharmaceutics, College of Pharmacy, The Ohio State University, Columbus, OH 43210

[‡]NSF Nanoscale Science and Engineering Center (NSEC) for Affordable Nanoengineering of Polymeric Biomedical Devices (CANPBD), The Ohio State University, Columbus, OH 43210

[§]Department of Chemical and Biomolecular Engineering, The Ohio State University, Columbus, OH 43210

[‖]Comprehensive Cancer Center (CCC), The Ohio State University, Columbus, OH 43210

[⊥]Department of Molecular Virology, Immunology and Medical Genetics, College of Medicine, The Ohio State University, Columbus, OH 43210

Abstract

Antisense oligonucleotide G3139 is designed for Bcl-2 downregulation and is known to induce toll-like receptor activation. Novel stabilized lipid-polycation-DNA (sLPD) nanoparticles were constructed and evaluated for the delivery of G3139 to human carcinoma KB cells and for bioactivity in *vivo*. Polyethylenimine (PEI) was incorporated as a DNA condensing agent. The lipid composition used was DOTAP/DDAB/Chol/TPGS/linoleic acid/hexadecenal at molar ratios of 30/30/34/1/5/0.2. The nanoparticles were stabilized by the formation of a reversible covalent bond between the aldehyde group on the cis-11-hexadecenal and amines on the PEI. When sLPDs were used to transfect KB cells, 90.4% Bcl-2 downregulation was observed, compared to no significant down-regulation by free G3139 and 54.6% down regulation by non-stabilized LPD-G3139. The sLPDs were then evaluated for therapeutic efficacy in mice bearing KB subcutaneous tumors and were found to trigger a strong antitumor response, inhibiting tumor growth and prolonging survival with 72% increase in lifespan (ILS). Consistent with previous reports on other G3139 nanoparticles, the increased anti-tumor activities of sLPDs in vivo were found to be associated with increased cytokine induction rather than Bcl-2 down-regulation, suggesting an immunological mechanism.

Keywords

Nanoparticles; antisense oligonucleotide; reversible crosslinking; cancer; immunotherapy; drug delivery

1. Introduction

Antisense oligodeoxyribonucleotides (ODNs), typically 15–20 nucleotides in length, are designed to specifically down-regulate targeted genes.[1] Meanwhile, ODNs, especially ODN

[*]To whom correspondence should be addressed. Robert J. Lee, College of Pharmacy, 500 W 12th Ave, Columbus, OH 43210; Tel: 614-292-4172; Fax: 614-292-7766; lee.1339@osu.edu.

NIH-PA Author Manuscript
NIH-PA Author Manuscript
NIH-PA Author Manuscript

NIH-PA Author Manuscript

NIH-PA Author Manuscript

NIH-PA Author Manuscript

nanoparticles, have been shown to induce toll-like receptor (TLR) activation in *vivo*, which leads to activation of genes such as Bcl-2. Free ODNs are rapidly cleared from circulation and lack a mechanism for crossing the cellular membrane.[2,3] To facilitate their delivery, cationic polymers, cationic lipids, and their combination have been used as delivery agents for ODNs by forming polyplexes, liposomes, or other types of nanoparticles.[2,4–8] These protect ODNs from nuclease degradation, promote cationic charge-mediated cellular uptake, and facilitate endosomal escape. Lipid-polycation-DNA (LPD) nanoparticles,[9] comprising ternary complexes of lipids, cationic polymer, and nucleic acid, have shown promise in ODN delivery.[8,10] The nanoparticle components can also enhance the TLR mediated immunomodulatory effects of ODN. In this study, a covalently stabilized form of LPD (sLPD) was synthesized based on reversible crosslinking of the cationic polymer polyethylenimine (PEI) with a reactive lipophilic component, cis-11-hexadecenal. The nanoparticles were studied for the delivery of ODN G3139 (Genasense™, oblimersen sodium), which targets the anti-apoptotic protein Bcl-2,[11,12] and were characterized for stability and biological activities both *in vitro* and *in vivo*. The immunomodulatory effects and antitumor therapeutic activity of the sLPD nanoparticles were investigated.

2. Materials and methods

2.1. Reagents

1,2-Dioleoyl-3-trimethylammonium-propane (DOTAP) was purchased from Avanti Polar Lipids (Alabaster, AL). Cholesterol (Chol), polyethylenimine (MW 2000) (PEI-2k), cis-11-hexadecenal, dimethyldioctadecylammonium bromide (DDAB), and D-α-tocopherol polyethylene glycol succinate (TPGS) were purchased from Sigma-Aldrich Chemical Co. (St. Louis, MO). All tissue culture media and supplies were purchased from Invitrogen (Carlsbad, CA).

2.2. Antisense oligonucleotides

Oligonucleotides used in this study were fully phosphorothioated. These include G3139 (5′-TCT CCC AGC GTG CGC CAT-3′) and fluorescein-labeled FAM-G3139, which were custom synthesized by Alpha-DNA (Montreal, QC, Canada).

2.3. Cell culture

Human carcinoma KB cells were cultured in RPMI 1640 media supplemented with 10% fetal bovine serum (FBS) (Invitrogen), 100 U/mL penicillin and 100 μg/mL streptomycin at 37 °C in a humidified atmosphere containing 5% CO_2.

2.4. Preparation of G3139-containing sLPDs

A modified ethanol dilution method[13] was used for the synthesis of sLPDs containing G3139. Briefly, a lipid mixture of DOTAP/DDAB/Chol/TPGS/linoleic acid/hexadecenal at molar ratios of 30/30/34/1/5/0.2 was dissolved in ethanol (EtOH) and quickly injected into an aqueous solution containing PEI-2k and $CaCl_2$. The above mixture was then quickly injected into G3139 dissolved in HEPES-buffered saline (HBS, composed of 20 mM HEPES, 145 mM NaCl, pH 7.4) at a ratio for total lipid:G3139 of 10:1 (w/w). This was followed by brief sonication to produce the final sLPD suspension with 50 μg/mL G3139 in 20% EtOH. The EtOH was then removed by dialysis against HBS using a MWCO 10,000 Dalton Float-A-Lyzer.

The particle size of sLPDs was analyzed using a NICOMP Particle Sizer Model 370 (Particle Sizing Systems, Santa Barbara, CA). All measurements were carried out in triplicate.

NIH-PA Author Manuscript

NIH-PA Author Manuscript

NIH-PA Author Manuscript

2.5. Measurement of colloidal and serum stability of sLPDs

The colloidal stability of sLPDs was evaluated by monitoring changes in their mean particle diameter during storage at 4 °C. To evaluate the ability of the sLPDs to retain G3139 and protect it against nuclease degradation, the formulation was mixed with FBS at a 1:4 (v/v) ratio and then incubated at 37 °C. At various time points, aliquots of each sample were loaded onto a 3% low melting point agarose gel. Electrophoresis was performed and the G3139 bands were visualized by ethidium bromide staining. The densities of G3139 band were measured and analyzed by the ImageJ software.

2.6. Cellular uptake of sLPD-G3139

Cellular uptake of sLPDs-G3139, spiked with 10% fluorescent oligonucleotide FAM-G3139, was evaluated in KB cells. For the studies, 4×10^5 cells were incubated with 500 nM sLPDs-G3139 at 37 °C. After 4-hr incubation, the cells were suspended by trypsin and washed three times with PBS by pelleting of the cells at 1,000× g for 3 min., followed by aspiration of the supernatant and re-suspension of the cells in PBS. The cells were examined on a Nikon fluorescence microscope (Nikon, Küsnacht, Switzerland). In addition, some cells were stained with 4′,6-diamidino-2-phenylindole (DAPI), a nuclear stain, and then examined on a Zeiss 510 META Laser Scanning Confocal Microscope (Carl Zeiss Inc., Germany).

2.7. Transfection studies

KB cells were seeded in 6-well tissue culture plates at 10^6/well in RPMI 1640 medium containing 10% FBS and were incubated at 37 °C overnight. sLPDs-G3139 or control formulations were then added into each well. After 4-hr incubation at 37 °C, fresh medium containing 10% FBS was added. The cells were incubated for another 48 hrs and then analyzed for Bcl-2 protein level by Western blot.

2.8. Quantification of Bcl-2 protein level by Western blot

Western blot was carried out to evaluate Bcl-2 expression at the protein level, as described previously.[8] Briefly, untreated and ODN-treated cells were incubated with a lysis buffer containing a protease inhibitor cocktail (CalBiochem, San Diego, CA) on ice for 20 min.. This was followed by collection of supernatant by centrifugation and determination of the protein concentrations by the BCA assay (Pierce, Rockford, IL). Proteins were then separated on a 15% Ready Gel Tris–HCl polyacrylamide gel (Bio-Rad, Hercules, CA), followed by transfer to a PVDF membrane. After blocking with 5% non-fat dry milk, the membranes were hybridized with monoclonal murine anti-human Bcl-2 (Dako, Carpinteria, CA) or polyclonal goat anti-human actin antibody (Santa Cruz Biotechnology, Santa Cruz, CA) and then with horseradish peroxidase-conjugated secondary antibodies. Membrane was then developed with Pierce SuperSignal West Dura Extended Duration Substrate (Pierce, Rockford, IL) and imaged with Kodak X-OMAT film (Kodak, Rochester, NY). Bcl-2 protein expression levels were quantified by ImageJ software (NIH Image, Bethesda, MD) and normalized to β-actin levels from the same samples.

2.9. Analysis of apoptosis by caspase activation

To analyze cellular apoptosis, caspase-9, caspase-3 and caspase-8 activities were measured on untreated-, LPD- and sLPD-treated cells, respectively, using the caspase colorimetric assay kits (R&D Systems, Minneapolis, MN). Briefly, 2×10^6 cells were collected and lysed and the reaction buffer and caspase colorimetric substrate were then added sequentially. After 60 min. at room temperature, the reaction mixtures were transferred to a 96-well microplate and read on a microplate reader at the wavelength of 405 nm. Differences in

NIH-PA Author Manuscript

NIH-PA Author Manuscript

NIH-PA Author Manuscript

caspase activity in sLPD-treated cells compared with control cells were determined by fold-change in the readout.

2.10. Evaluation of anti-tumor activity

Female athymic (HSD:Athymic nude-FOXN1nd) mice were purchased from Harlan (Indianapolis, IN). For the xenograft model, KB cells (5×10^6) were subcutaneously inoculated into the flank of the mice. Palpable tumors developed within 4–5 days after inoculation. At 5 days post inoculation, the tumor-bearing mice were injected i.v. with PBS (pH 7.4), free G3139 or sLPD-G3139 at G3139 dose of 5 mg/kg on every 3rd day. Empty LPD and sLPD without ODN were also included as control treatments. Five mice were used in each treatment group. Anti-tumor activity was determined by measuring the tumor size (width and length) using a Vernier caliper at a series of time points. Tumor volume was calculated by the formula: tumor volume = 1/2 × length (mm) × (width (mm))^2. Mice were scarified once the tumor size reached greater than 1,500 mm^3.

2.11. *In vivo* tumor localization of sLPD-G3139

To evaluate *in vivo* tumor accumulation,[14] FAM-G3139 loaded sLPD was administered at 5 mg/kg ODN dose into tumor-bearing mouse by tail vein injection. Tumors were harvested at various time points and homogenized in microtubes containing 500 μL distilled water. Samples were then treated with 1% SDS, and heated at 95 °C for 5 min., followed by centrifugation at 12,000 × g for 5 min. The fluorescence intensity of the supernatant was determined on a spectrofluorometer (PerkinElmer, Boston, MA) to determine sample ODN concentration.

2.13. Immunohistochemical analysis of Bcl-2 expression in tumor

For immunohistochemical analysis,[14] tumor samples after 4 treatments were fixed with 4% PBS-buffered formalin and rinsed for 3 times with PBS. These were then embedded in paraffin, sectioned using a microtone, placed on siliconized glass slides and then air-dried. Then, the slides were de-paraffinized and treated with 3% hydrogen peroxide in methanol. The slides were then rinsed 3 times with PBS and blocked for 2 hrs at room temperature with 1% normal goat serum in PBS. Bcl-2 was stained by firstly incubating the slides with primary rabbit antibody against human Bcl-2 (Santa Cruz Biotechnology) at 1:200 dilution. The slides were then washed 3 times with PBS, treated with biotinylated anti-rabbit IgG and incubated at room temperature for 1 hr. Finally, the samples were counterstained with hematoxylin and eosin (H&E), dehydrated, and mounted with Permount. Slides with H&E staining only were used as control.

2.14. Evaluation of cytokine production

To evaluate the immune response of the mice to sLPD treatment, serum IFN-γ and IL-6 levels in tumor-bearing mice were measured. Briefly, 4 hr after sLPD-G3139 injection in to mice, blood was collected and serum was isolated by centrifugation at 12,000× g. Control treatment groups included PBS, free G3139 and non-stabilized LPD-G3139. Cytokine levels were determined using commercial ELISA kits for murine IFN-γ (BD Pharmingen, San Diego, CA) and murine IL-6 (eBioscience, San Diego, CA).

2.15. Statistical analysis

Data obtained were shown as mean ± standard deviation (SD). Comparisons between groups were made by 2-tailed Student's t-tests using the MiniTAB software (Minitab Inc., State College, PA). Differences in survival of mice among treatment groups were analyzed using the log-rank test. $p < 0.05$ was used as the cutoff for defining statistically significant differences.

NIH-PA Author Manuscript

NIH-PA Author Manuscript

NIH-PA Author Manuscript

3. Results

3.1. Physical chemical properties of sLPD-G3139

The sLPD was prepared by a modified ethanol injection method, as described in Materials and Methods. It was composed of lipids DOTAP and DDAB, cholesterol, TPGS, linoleic acid and hexadecenal. PEI-2k and Ca^{2+} were added to facilitate ODN condensation and enhance the oligonucleotide delivery. The hexadecenal was included to increase the particle stability via formation of a reversible covalent bond between hexadecenal in the lipid bilayer and an amine on the PEI-2k (Figure 1A). The final formulation was defined as sLPD. The sLPD-G3139 has the composition of lipids, PEI-2k, $CaCl_2$ and G3139, at the weight ratio of lipid/PEI/ODN of 10:0.5:1, final ODN concentration of 20 μM and $CaCl_2$ concentration of 2 mM. The lipid composition used was DOTAP/DDAB/Chol/TPGS/linoleic acid/hexadecenal at molar ratios of 30:30:34:1:5:0.2. The structure of sLPD was schematically presented in Figure 1B. We propose that during its synthesis, cationic components are first combined. The nanoparticles are assembled upon the injection of the negatively charged G3139. Due to the small size (faster diffusion) and high charge density of PEI-2k, G3139 should initially form complexes with PEI-2k, stabilized by Ca^{2+}. This is then further stabilized by further complexation with the cationic liposomes in the mixture and the formation of a lipid bilayer coating. The final assembled sLPD is stabilized by the reaction between hexadecenal on the lipid bilayer and the PEI-2k.

The sLPD particles had a particle size of 105.4±10.3 nm, similar to that of LPD (108.8±7.3 nm), as shown in Table 1. The effects of PEI-2k and Ca^{2+} on particle size were evaluated as well. Without PEI-2k, the particle size was larger at 147.3±8.5 nm, indicating an important role for PEI-2k in DNA condensation. The presence of Ca^{2+} in the formulation did not affect the particle size significantly. The particle sizes were below 200 nm and sterically stabilized by TPGS, therefore may exhibit long circulation and the enhanced permeability and retention (EPR) effect *in vivo*.

3.2. Stability of sLPD-G3139

The colloidal stability of sLPD-G3139 was evaluated by monitoring changes in its mean diameter over time. As shown in Figure 2A, sLPDs remained stable at both 4 °C and the room temperature for 8 weeks. In contrast, although LPDs maintained small particle size over storage at 4 °C, the size increased to >350 nm at the 4^{th} week when kept at the room temperature. To evaluate its ability to protect oligos against nuclease degradation, sLPD-G3139 was mixed with FBS at a 1:4 (v/v) ratio and incubated at 37 °C. At various incubation time points, aliquots of each sample were loaded onto a 3% low melting point agarose gel. Electrophoresis was performed and G3139 was visualized under UV after ethidium bromide staining. As shown in Figure 2B, the amount of intact G3139 remaining in the particles decreased over time. After 8-hr exposure to serum, ~ 76% of G3139 remained in the sLPD sample whereas no unformulated G3139 and LPD-loaded G3139 remained, indicating that sLPD nanoparticles protected ODNs against serum DNase degradation and therefore have greater serum stability than the traditional LPD formulation.

3.3. sLPD mediated cellular uptake of G3139

Uptake of sLPD-G3139 (containing 10% fluorescent FAM-G3139) was evaluated in KB cells under a confocal microscope. The cell nuclei were stained by DAPI. As shown in Figure 3A, there was significant cellular uptake, including internalization, of the sLPDs. At the 240 min. time point., nuclei in some of the cells appeared fragmented, indicating the occurrence of apoptosis in these cells (Figure 5A). To differentiate the ODNs in cytoplasm from those distributed in the nuclei, optical sections (total 14) of cells at 4 hr were scanned along the z-axis at an increment of 0.45 μm, as shown in Figure 3B. FAM-ODN mostly

NIH-PA Author Manuscript

NIH-PA Author Manuscript

NIH-PA Author Manuscript

remained in the endosomal compartments. Compared to free G3139 and LPD-G3139 formulations, sLPD-G3139 showed much higher level of cellular uptake and more efficient internalization when visualized on a fluorescence microscope (Figure 3C).

3.4. Effect of sLPD-G3139 on Bcl-2 expression

KB cells were transfected with sLPD-G3139 in presence of 10% serum. After 48-hr incubation, cellular protein was extracted and Western blot was performed to determine Bcl-2 protein expression level. Stabilized sLPD formulation showed higher biological activity than the non-stabilized traditional LPD formulation. As shown in Figure 4A, there was 90.4% Bcl-2 down-regulation by G3139 in sLPDs while LPD-G3139 induced only 54.6% Bcl-2 down-regulation. Meanwhile free G3139 did not impact Bcl-2 expression. We also found that the inhibition of Bcl-2 expression by sLPD-G3139 was concentration-dependent. A higher amount of sLPD-G3139 resulted in greater Bcl-2 down-regulation (Figure 4B).

3.5. sLPD-G3139 induction of cellular apoptosis

Having demonstrated knockdown of the anti-apoptotic protein Bcl-2, the *in vitro* pharmacological activity of sLPD-G3139 was further investigated by determining activities of caspase-9, 3 and 8 in KB cells. At 48 hrs after treatment, the cells were collected and analyzed by caspase assay. As shown in Figure 5, caspase-9 and caspase-3 activities in sLPD-G3139-treated cells were 2.1 × and 3.3 × higher, respectively, than that in cells treated with non-stabilized LPD-G3139. There was a 36-fold increase in caspase-3 activity in the sLPD treated group than that in free G3139 group, indicating markedly enhanced apoptosis induction by the sLPD-G3139. Regarding caspase-8, no induction was observed in free G3139 group while some induction was found in both sLPD and LPD groups. There was no significant difference in caspase-8 activity between the two groups. Empty nanoparticles did not significant induce apoptosis via either the caspase-3/9 pathway or the caspase-8 signal pathway.

3.6. Tumor suppression and survival prolongation by sLPD-G3139

sLPD-G3139s were studied for therapeutic efficacy in mice with xenograft KB tumors. The tumor model was established in nude mice by subcutaneous implantation with KB cells. The mice developed tumors of ~ 20 mm^3 within 5 days, which reached a size of >1,500 mm^3 within 1 month in the absence of treatment. For the therapeutic study, the mice were injected i.v. with sLPD-G3139 every 3 days starting from day 5 post inoculation. The control group mice were given PBS (pH 7.4) instead. As shown in Figure 6A, tumor growth in the mice treated with sLPD-G3139 was inhibited by > 67% ($p < 0.01$) at the end of the 1-month treatment, resulting in a doubling of the duration of survival (Figure 6B and Table 2). In contrast, neither free G3139 nor PBS had a significant effect on tumor growth and survival rate of tumor-bearing mice (Figure 6A and 6B). The mice treated with LPD-G3139 had much lower activities in mediating tumor suppression (36%) and lifespan increase (64%). Interestingly, empty sLPD also showed a significant anti-tumor activity while empty LPD did not.

3.7. G3139 accumulation and Bcl-2 expression in tumors

The antitumor activity of G3139 has been attributed to both down-regulation of Bcl-2 expression[11,12] and its immunomodulatory effects.[15] To investigate if tumor suppression by sLPD-G3139 was caused by the antisense effect, we evaluated the G3139 accumulation and Bcl-2 expression in tumor tissues treated by sLPD-G3139. The data showed that while LPD-G3139 reached its maximum concentration in tumor (6.2 μg G3139/g tumor) at 480 min.. after the administration, the sLPD-G3139 level in tumor reach its maximum of 11.3 μg

NIH-PA Author Manuscript

NIH-PA Author Manuscript

NIH-PA Author Manuscript

G3139/g tumor tissue at 24 hr after the administration. Therefore, the data indicated that both LPD and sLPD had much greater tumor delivery compared to free G3139, possibly due to the increased circulation time and the enhanced permeability and retention (EPR) effect. Rather than down-regulation, immunohistochemical staining results (Figure 7B) showed that Bcl-2 expression in tumors were significantly upregulated by sLPD-G3139 and LPD-G3139 compared to those that were treated with PBS or free G3139. A lower level of Bcl-2 induction was also observed in free G3139 treated mice.

3.8. Induction of cytokine production by sLPD-G3139

The immunomodulatory effects of sLPD-G3139 was studied by measuring cytokine production in treated mice. At 4 hrs after the treatment by sLPD-G3139 or controls (free G3139, LPD-G3139, empty LPD or empty sLPD), mice serum was collected and cytokine IL-6 and IFN-γ were determined by ELISA. As shown in Figure 8, sLPD-G3139 induced much higher immune responses compared to free G3139 ($p < 0.01$) with a 21-fold increase in IL-6 and 16-fold increase in IFN-γ levels. The empty sLPD also induced high cytokine production levels, indicating the sLPD components played an important role in the immune stimulation. Empty LPD showed the similar performance in inducing IL-6 production with empty sLPD, while it did not significantly enhance the IFN-γ production.

4. Discussion

In this study, hexadecenal was added in LPDs to form a reversible covalent bond with PEI-2k in the particle core, which promoted the stability of nanoparticles over storage and in serum. The C=N bond is reversible at acidic pH, which may facilitate release of ODN from nanoparticles inside the endosomes. When developing sLPD in this study, two cationic lipids DOTAP and DDAB were used in the same formulation, which was shown to reduce the cytotoxicity relative to single cationic lipids (unpublished data). Chol and TPGS were used to promote particle stability.[16–19] Linoleic acid was added due to its ability to promote bilayer phase transition to a non-bilayer structure upon protonation at endosomal pH, which contributes to endosomal escape of the ODN.[20] Ca^{2+}, in the form of phosphate salt, has been used in gene delivery[21–24] with limited efficiency compared to other cationic polymer/lipid-based nanoparticles. Recently, a lipid coated calcium phosphate (LCP) nanoparticle (NP) formulation was developed for efficient delivery of small interfering RNA (siRNA).[25] Our lab has also reported that a gene transfer vector comprising lipid-coated nano-calcium-phosphate (LNCP) could provide more efficient and satisfactory pDNA delivery.[26] In this study, Ca^{2+} was added for increasing sLPD stability.

sLPDs synthesized in this study showed very high ODN G3139 delivery efficiency in human carcinoma KB cell both *in vitro* and *in vivo*, evidenced by the results of increased G3139 cellular uptake, down-regulated Bcl-2 expression and induction of caspases *in vitro* and suppression of tumor growth *in vivo* and increased tumor localization. However, it seemed that the *in vivo* tumor suppression was not due to the G3139 antisense effect because the immunohistochemical experiments actually showed much higher expression of Bcl-2 after the treatment of tumor-bearing mice by sLPD-G3139 compared to those treated by the same amount of free G3139. It has been previously established that antisense ODN G3139 may function by both down-regulating Bcl-2 expression to induce cellular apoptosis[8,11,12,27] and sensitize cells to chemotherapy drugs,[28] and by activating the immune cells such as dendritic cells (DC), macrophages and natural killer (NK) cells, through its 2 CpG motifs and toll-like receptor 9 (TLR9) activation.[15,29,30] However, we noticed that free G3139 did not induce as much cytokine production as the same amount of sLPD-G3139, consistent with previous findings[15]. The lipid and polymer components in sLPD-G3139 and LPD-G3139 seemed to be important for the dramatic increase in cytokine production because G3139-loaded and empty LPDs also increased elevated IL-6 levels. It

NIH-PA Author Manuscript

NIH-PA Author Manuscript

NIH-PA Author Manuscript

has been reported that cationic lipids by themselves have limited immune stimulatory activity,[31] while they seem to enhance the immunomodulatory effects of unmethylated CpG in DNA ODN both *in vitro* and in vivo.[15,31,32,33] It is interesting that the sLPD alone triggered cytokine production. These findings are consistent with some previous reports.[34,35] It seems as that the immune activity of lipid-based nanoparticles depend on their specific composition and the corresponding surface chemistry. For example, the combination of cationic lipid and protamine had little effect on cytokine induction.[33] While in this study, the empty sLPD containing two cationic lipids, PEI-2k and calcium showed high cytokine production levels, about 65% of that induced by sLPD-ODN complex. Our data showed that the covalent stabilization in sLPD further increased TLR activation because sLPD-G3139 stimulated much higher IFN-γ than LPD-G3139.

In conclusion, sLPD is highly efficacious in G3139 delivery in vitro and therapeutically active against murine xenograft tumors in vivo. The mechanism of its antitumor activity appears to be based on its immunomodulatory effects. Nevertheless, the high potency of this activity suggests that sLPD-G3139 warrant further study as a potential therapeutic agent.

Acknowledgments

This work was supported by NSF grant EEC-0425626.

References

1. Crooke ST. Progress in antisense technology. Annu Rev Med. 2004; 55:61–95. [PubMed: 14746510]
2. Zhang C, Pei J, Kumar D, Sakabe I, Boudreau HE, Gokhale PC, Kasid UN. Antisense oligonucleotides: target validation development of systemically delivered therapeutic nanoparticles. Methods Mol Biol. 2007; 361:163–185. [PubMed: 17172711]
3. Shoji Y, Nakashima H. Current status of delivery systems to improve target efficacy of oligonucleotides. Curr Pharm Des. 2004; 10:785–796. [PubMed: 15032703]
4. Wheeler JJ, Palmer L, Ossanlou M, MacLachlan I, Graham RW, Zhang YP, Hope MJ, Scherrer P, Cullis PR. Stabilized plasmid-lipid particles: construction and characterization. Gene Ther. 1999; 6:271–281. [PubMed: 10435112]
5. Zaghloul EM, Viola JR, Zuber G, Smith CI, Lundin KE. Formulation and delivery of splice-correction antisense oligonucleotides by amino acid modified polyethylenimine. aMol Pharm. 2010; 7:652–663.
6. Junghans M, Kreuter J, Zimmer A. Antisense delivery using protamine-oligonucleotide particles. Nucleic Acids Res. 2000; 28:E45. [PubMed: 10773093]
7. Gao X, Huang L. Potentiation of cationic liposome-mediated gene delivery by polycations. Biochemistry. 1996; 35:1027–1036. [PubMed: 8547238]
8. Yang X, Koh CG, Liu S, Pan X, Santhanam R, Yu B, Peng Y, Pang J, Golan S, Talmon Y, Jin Y, Muthusamy N, Byrd JC, Chan KK, Lee LJ, Marcucci G, Lee RJ. Transferrin receptor-targeted lipid nanoparticles for delivery of an antisense oligodeoxyribonucleotide against Bcl-2. Mol Pharm. 2009; 6:221–230. [PubMed: 19183107]
9. Li S, Huang L. In vivo gene transfer via intravenous administration of cationic lipid-protamine-DNA (LPD) complexes. Gene Ther. 1997; 4:891–900. [PubMed: 9349425]
10. Junghans M, Loitsch SM, Steiniger SC, Kreuter J, Zimmer A. Cationic lipid-protamine-DNA (LPD) complexes for delivery of antisense c-myc oligonucleotides. Eur J Pharm Biopharm. 2005; 60:287–294. [PubMed: 15939239]
11. Klasa RJ, Gillum AM, Klem RE, Frankel SR. Oblimersen Bcl-2 antisense: facilitating apoptosis in anticancer treatment. Antisense Nucleic Acid Drug Dev. 2002; 12:193–213. [PubMed: 12162702]
12. Marcucci G, Stock W, Dai G, Klisovic RB, Liu S, Klisovic MI, Blum W, Kefauver C, Sher DA, Green M, Moran M, Maharry K, Novick S, Bloomfield CD, Zwiebel JA, Larson RA, Grever MR, Chan KK, Byrd JC. Phase I study of oblimersen sodium an antisense to Bcl-2 in untreated older

NIH-PA Author Manuscript

NIH-PA Author Manuscript

NIH-PA Author Manuscript

patients with acute myeloid leukemia: pharmacokinetics pharmacodynamics clinical activity. J Clin Oncol. 2005; 23:3404–3411. [PubMed: 15824414]

13. Jeffs LB, Palmer LR, Ambegia EG, Giesbrecht C, Ewanick S, MacLachlan I. A scalable, extrusion-free method for efficient liposomal encapsulation of plasmid DNA. Pharm Res. 2005; 22:362–372. [PubMed: 15835741]
14. Zhang X, Koh CG, Yu B, Liu S, Piao L, Marcucci G, Lee RJ, Lee LJ. Transferrin receptor targeted lipopolyplexes for delivery of antisense oligonucleotide g3139 in a murine k562 xenograft model. Pharm Res. 2009; 26:1516–1524. [PubMed: 19291371]
15. Pan X, Chen L, Liu S, Yang X, Gao JX, Lee RJ. Antitumor activity of G3139 lipid nanoparticles (LNPs). Mol Pharm. 2009; 6:211–220. [PubMed: 19072654]
16. Ogihara-Umeda I, Kojima S. Cholesterol enhances the delivery of liposome-encapsulated gallium-67 to tumors. Eur J Nucl Med. 1989; 15:612–617. [PubMed: 2598958]
17. Somavarapu S, Pandit S, Gradassi G, Bandera M, Ravichandran E, Alpar OH. Effect of Vitamin E TPGS on immune response to nasally delivered diphtheria toxoid loaded poly(caprolactone) microparticles. Int J Pharm. 2005; 298:344–347. [PubMed: 15967606]
18. Feng SS, Huang GF. Effects of emulsifiers on the controlled release of paclitaxel (Taxol (R)) from nanospheres of biodegradable polymers. J Control Release. 2001; 71:53–69. [PubMed: 11245908]
19. Mu L, Feng SS. Vitamin E TPGS used as emulsifier in the solvent evaporation/extraction technique for fabrication of polymeric nanospheres for controlled release of paclitaxel (Taxol (R)). J Control Release. 2002; 80:129–144. [PubMed: 11943393]
20. Shigeta Y, Imanaka H, Ando H, Ryu A, Oku N, Baba N, Makino T. Skin whitening effect of linoleic acid is enhanced by liposomal formulations. Biol Pharm Bull. 2004; 27:591–594. [PubMed: 15056874]
21. Orrantia E, Chang PL. Intracellular distribution of DNA internalized through calcium phosphate precipitation. Exp Cell Res. 1990; 190(2):170–174. [PubMed: 2209719]
22. Batard P, Jordan M, Wurm F. Transfer of high copy number plasmid into mammalian cells by calcium phosphate transfection. Gene. 2001; 270:61–68. [PubMed: 11404003]
23. Roy I, Mitra S, Maitra A, Mozumdar S. Calcium phosphate nanoparticles as novel non-viral vectors for targeted gene delivery. Int J Pharm. 2003; 250:25–33. [PubMed: 12480270]
24. Bisht S, Bhakta G, Mitra S, Maitra A. pDNA loaded calcium phosphate nanoparticles: highly efficient non-viral vector for gene delivery. Int J Pharm. 2005; 288:157–168. [PubMed: 15607268]
25. Li J, Chen YC, Tseng YC, Mozumdar S, Huang L. Biodegradable calcium phosphate nanoparticle with lipid coating for systemic siRNA delivery. J Control Release. 2010; 142:416–421. [PubMed: 19919845]
26. Zhou C, Yu B, Yang X, Huo T, Lee LJ, Barth RF, Lee RJ. Lipid-coated nano-calcium-phosphate (LNCP) for gene delivery. Int J Pharm. 2010; 392:201–208. [PubMed: 20214964]
27. Dai G, Chan KK, Liu S, Hoyt D, Whitman S, Klisovic M, Shen T, Caligiuri MA, Byrd J, Grever M, Marcucci G. Cellular uptake and intracellular levels of the bcl-2 antisense g3139 in cultured cells and treated patients with acute myeloid leukemia. Clin Cancer Res. 2005; 11(8):2998–3008. [PubMed: 15837754]
28. Moore J, Seiter K, Kolitz J, Stock W, Giles F, Kalaycio M, Zenk D, Marcucci G. A Phase II study of Bcl-2 antisense (oblimersen sodium) combined with gemtuzumab ozogamicin in older patients with acute myeloid leukemia in first relapse. Leuk Res. 2006; 30:777–783. [PubMed: 16730060]
29. Gekeler V, Gimmnich P, Hofmann HP, Grebe C, Römmele M, Leja A, Baudler M, Benimetskaya L, Gonser B, Pieles U, Maier T, Wagner T, Sanders K, Beck JF, Hanauer G, Stein CA. G3139 and other CpG-containing immunostimulatory phosphorothioate oligodeoxynucleotides are potent suppressors of the growth of human tumor xenografts in nude mice. Oligonucleotides. 2006; 16(1):83–93. [PubMed: 16584297]
30. Krieg AM. CpG motifs in bacterial DNA and their immune effects. Annu Rev Immunol. 2002; 20:709–760. [PubMed: 11861616]
31. Dow SW, Fradkin LG, Liggitt DH, Willson AP, Heath TD, Potter TA. Lipid-DNA complexes induce potent activation of innate immune responses antitumor activity when administered intravenously. J Immunol. 1999; 163(3):1552–1561. [PubMed: 10415059]

NIH-PA Author Manuscript

NIH-PA Author Manuscript

NIH-PA Author Manuscript

32. Mui B, Raney SG, Semple SC, Hope MJ. Immune stimulation by a CpG-containing oligodeoxynucleotide is enhanced when encapsulated and delivered in lipid particles. J Pharmacol Exp Ther. 2001; 298 (3):1185–1192. [PubMed: 11504819]
33. Gursel I, Gursel M, Ishii KJ, Klinman DM. Sterically stabilized cationic liposomes improve the uptake and immunostimulatory activity of CpG oligonucleotides. J Immunol. 2001; 167 (6):3324–3328. [PubMed: 11544321]
34. Cui Z, Han SJ, Vangasseri DP, Huang L. Immunostimulation mechanism of LPD nanoparticle as a vaccine carrier. Mol Pharm. 2005; 2(1):22–28. [PubMed: 15804174]
35. Dobrovolskaia MA, McNeil SE. Immunological properties of engineered nanomaterials. Nat Nanotechnol. 2007; 2(8):469–478. [PubMed: 18654343]
36. Krieg AM. Therapeutic potential of Toll-like receptor 9 activation. Nat Rev Drug Discov. 2006; 5(6):471–484. [PubMed: 16763660]
37. Iwasaki A, Medzhitov R. Toll-like receptor control of the adaptive immune responses. Nat Immunol. 2004; 5(10):987–995. [PubMed: 15454922]
38. Maurer N, Mori A, Palmer L, Monck MA, Mok KW, Mui B. Lipid-based systems for the intracellular delivery of genetic drugs. Mol Membr Biol. 1999; 16(1):129–140. [PubMed: 10332748]
39. Li B, Li S, Tan Y, Stolz DB, Watkins SC, Block LH. Lyophilization of cationic lipid-protamine-DNA (LPD) complexes. J Pharm Sci. 2000; 89(3):355–364. [PubMed: 10707016]
40. Wiethoff CM, Middaugh CR. Barriers to nonviral gene delivery. J Pharm Sci. 2003; 92(2):203–217. [PubMed: 12532370]
41. Mu L, Feng SS. PLGA/TPGS nanoparticles for controlled release of paclitaxel: effects of the emulsifier and drug loading ratio. Pharm Res. 2003; 20:1864–1872. [PubMed: 14661934]
42. Mu L, Feng SS. A novel controlled release formulation for the anticancer drug paclitaxel (Taxol (R)): PLGA nanoparticles containing vitamin E TPGS. J Control Release. 2003; 86:33–48. [PubMed: 12490371]
43. Fischer JR, Harkin KR, Freeman LC. Concurrent administration of water-soluble vitamin E can increase the oral bioavailability of cyclosporine A in healthy dogs. Vet Tech: Res Appl Vet Med. 2002; 3:465–473.
44. Dintaman JM, Silverman JA. Inhibition of P-glycoprotein by D-alpha-tocopheryl polyethylene glycol 1000 succinate (TPGS). Pharm Res. 1999; 16:1550–1556. [PubMed: 10554096]
45. Yu L, Bridgers A, Polli J. Vitamin E-TPGS increases absorption flux of an HIV protease inhibitor by enhancing its solubility and permeability. Pharm Res. 1999; 16:1812–1817. [PubMed: 10644067]
46. Rege BD, Kao JPY, Polli JE. Effects of nonionic surfactants on membrane transporters in Caco-2 cell monolayers. Eur J Pharm Sci. 2002; 16:237–246. [PubMed: 12208453]
47. Schmidt HT, Ostafin AE. Liposome directed growth of calcium phosphate nanoshells. Adv Mater. 2002; 14:532–535.
48. Cheson BD. Oblimersen for the treatment of patients with chronic lymphocytic leukemia. Ther Clin Risk Manag. 2007; 3:855–870. [PubMed: 18473009]

NIH-PA Author Manuscript

NIH-PA Author Manuscript

NIH-PA Author Manuscript

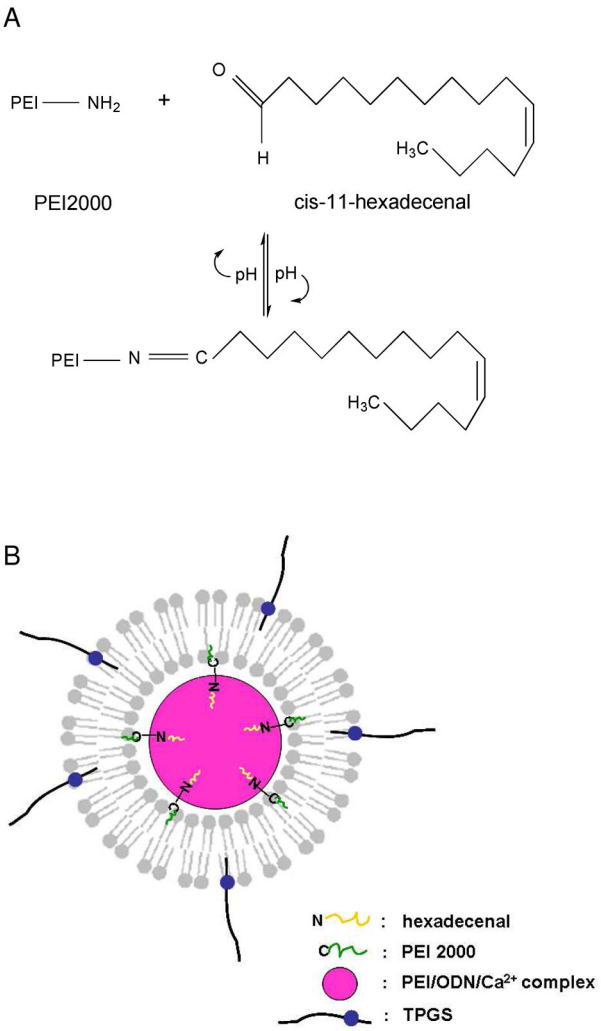

Figure 1.
Design of sLPD
Panel A. Formation of a Schiff's base between PEI-2k and hexadecenal.
Panel B. A model for the structure of sLPD

NIH-PA Author Manuscript

NIH-PA Author Manuscript

NIH-PA Author Manuscript

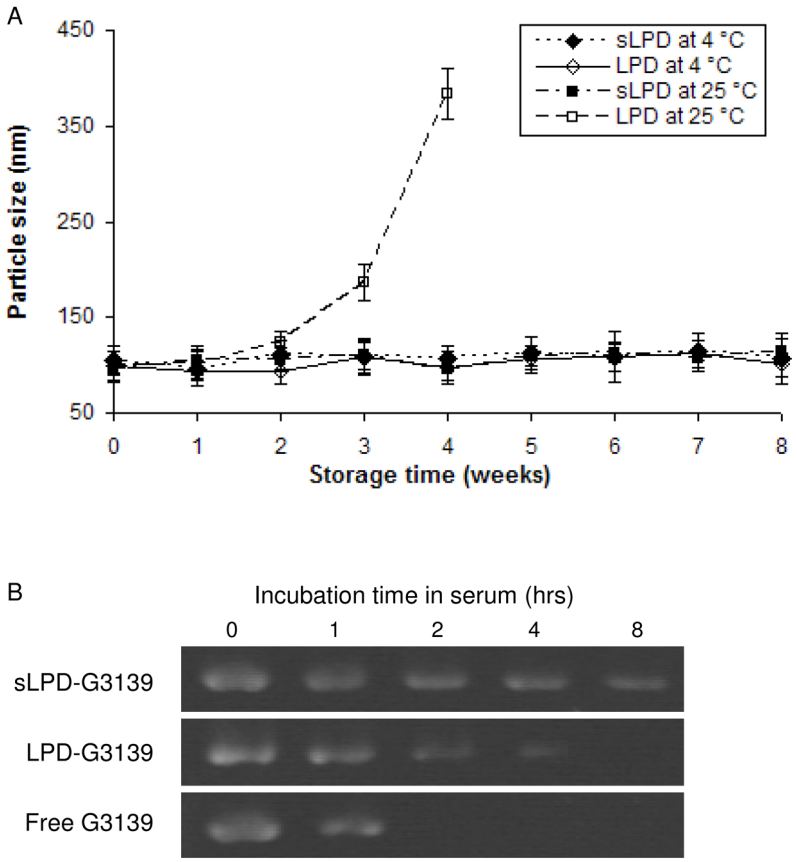

Figure 2.
Colloidal and serum stability of sLPD
Panel A. Colloidal stability of sLPDs.
Panel B. Stability of sLPD-G3139 in serum. The sLPD-G3139 was mixed with serum at 1:4 volume ratio and incubated at 37 °C for different times. The samples were then analyzed by electrophoresis in 3% low melting point agarose gel and stained with ethidium bromide.

NIH-PA Author Manuscript

NIH-PA Author Manuscript

NIH-PA Author Manuscript

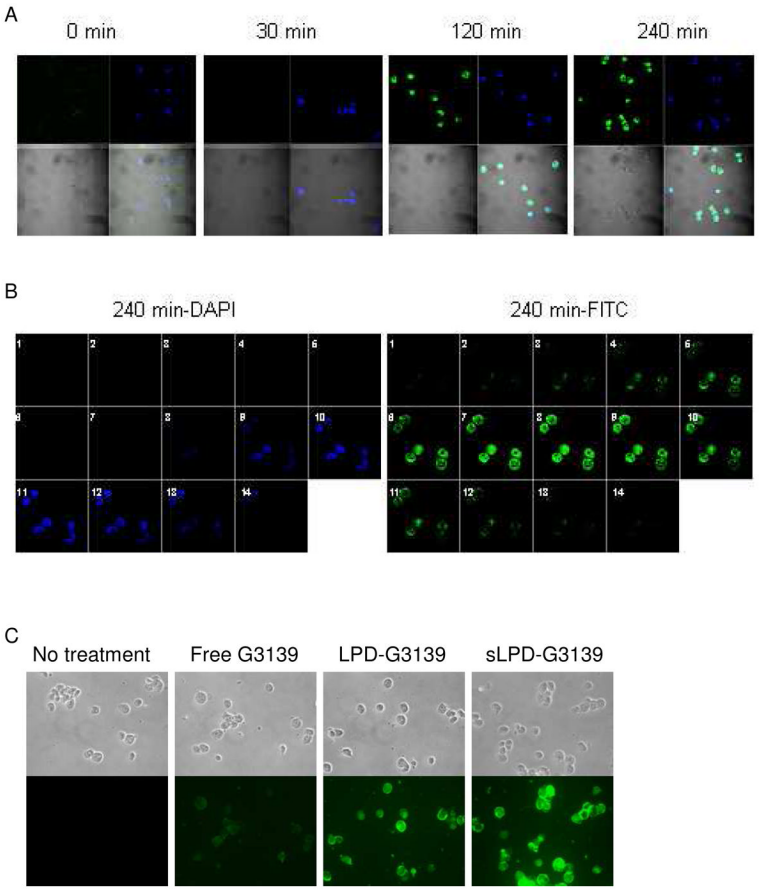

Figure 3.

Internalization of sLPD-G3139 in KB cells

The cells were incubated with 500 nM sLPD-G3139 (containing 10% fluorescent FAM-G3139) at 37 °C. At different time points, unbound sLPDs were removed by washing with PBS and cellular nuclei were stained by DAPI. The cell were then mounted to the slide and observed under a fluorescence microscope. Blue color indicated nuclei stained by DAPI and green color indicated FAM-labeled G3139.

Panel A. Cells were treated with sLPD-G3139 spiked with 10% FAM-G3139 (green) at 37°C for 30, 120 and 240 min., respectively, stained by DAPI (blue) and visualized on a confocal microscope.

Panel B. Optical sections (14 total) of cells were collected after 4 hr by incremental scanning along the z-axis at a spacing of 0.45 μm.

Panel C. Cells were treated with sLPD-G3139 and visualized on a fluorescence microscope.

NIH-PA Author Manuscript

NIH-PA Author Manuscript

NIH-PA Author Manuscript

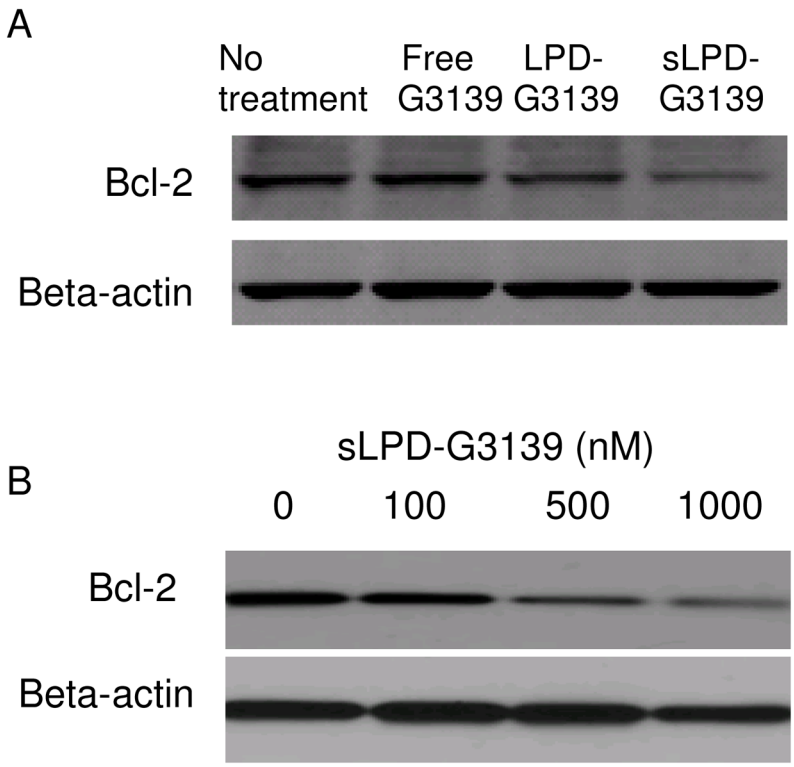

Figure 4.
Bcl-2 protein expression in KB cells treated with sLPD-G3139
Panel A. Bcl-2 down-regulation by Western blot. Cells were treated with PBS, free G3139 or sLPD-G3139 at 1 μM. Bcl-2 protein levels were analyzed at 48 hrs by Western blot. Upper panel represents the results of Western blot and lower represents its corresponding densitometry data.
Panel B. Concentration-dependent Bcl-2 down-regulation by sLPD-G3139.
Cells were treated with sLPD-G3139 at different concentrations. Bcl-2 protein levels were analyzed at 48 hrs by Western blot. Upper panel shows the results of Western blot and lower its corresponding densitometry data.

NIH-PA Author Manuscript

NIH-PA Author Manuscript

NIH-PA Author Manuscript

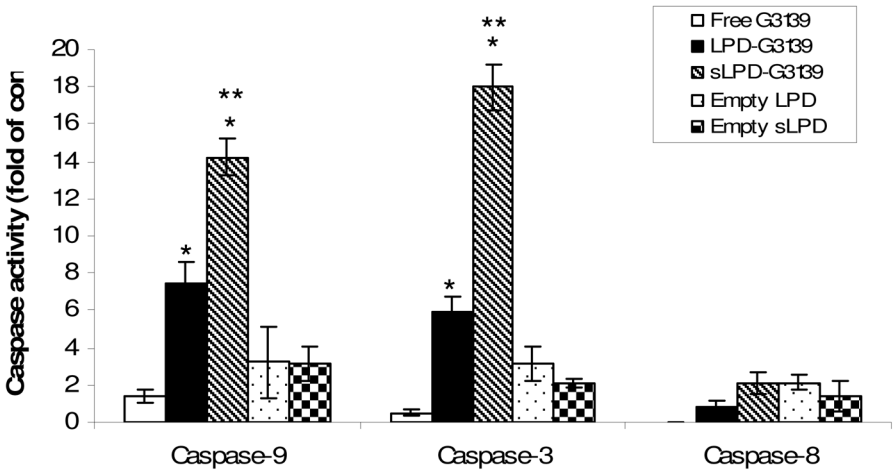

Figure 5.

Induction of caspases in KB cells treated with sLPD-G3139. Cells were incubated 1 μM sLPD-G3139 or control formulations. Cellular apoptosis was evaluated via caspase-9, -3 and -8 activities, as described in the Materials and Methods section. The values in the plot represent the means of 4 separate experiments. Error bars were standard deviations, n=4. *, $p < 0.05$, when compared to the free G3139 group. **, $p < 0.05$, when compared to the LPD-G3139 group.

NIH-PA Author Manuscript
NIH-PA Author Manuscript
NIH-PA Author Manuscript

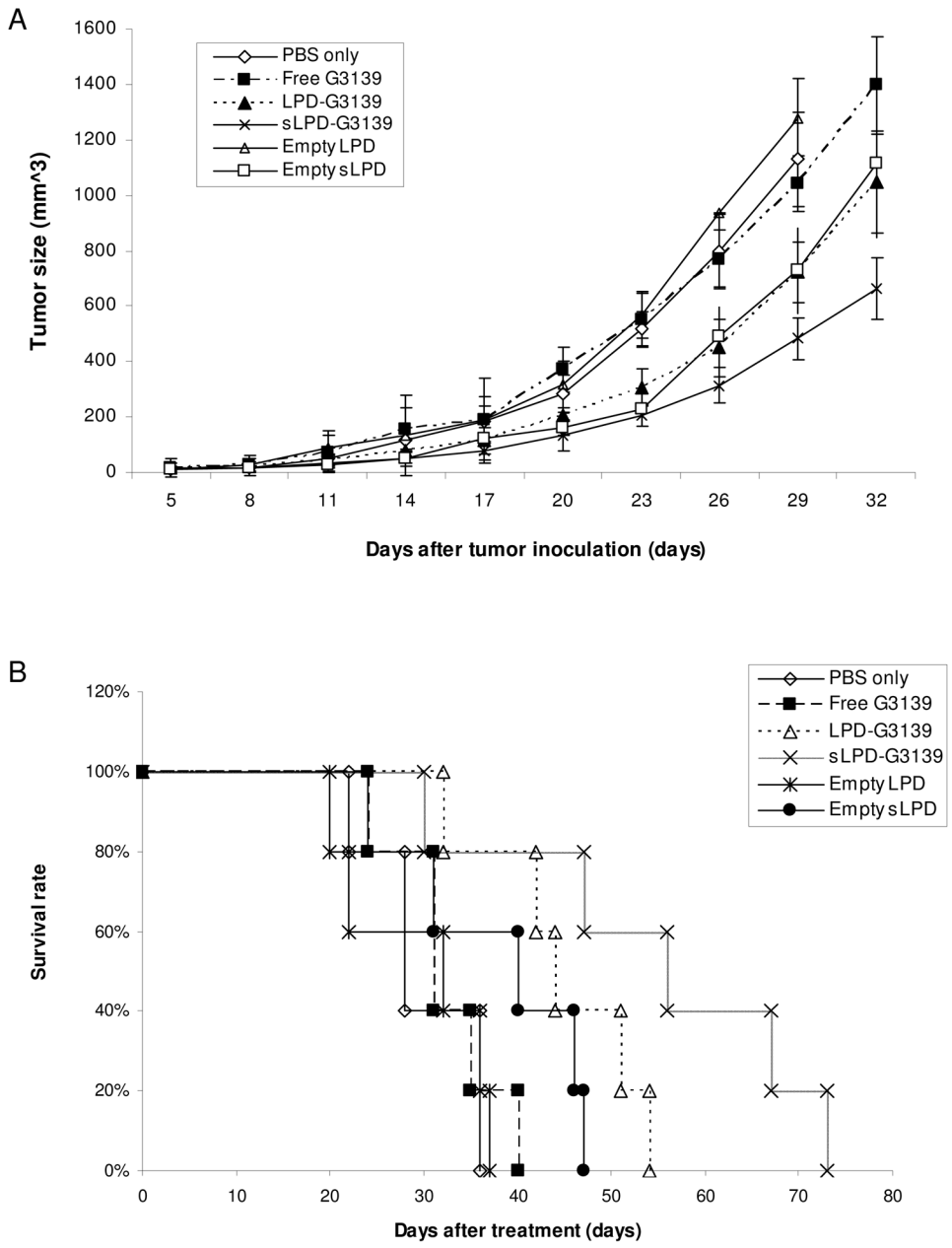

Figure 6.

Therapeutic efficacy of sLPD-G3139s

Nude mice were inoculated s.c. with human KB cells 5 days prior to treatment. The mice received i.v. injections of 5mg/kg sLPD-G3139 or control formulations on every 3rd day. Five mice were used in each group.

Panel A. Effect of treatment on tumor size. **Panel B.** Effect of treatment on animal survival.

NIH-PA Author Manuscript

NIH-PA Author Manuscript

NIH-PA Author Manuscript

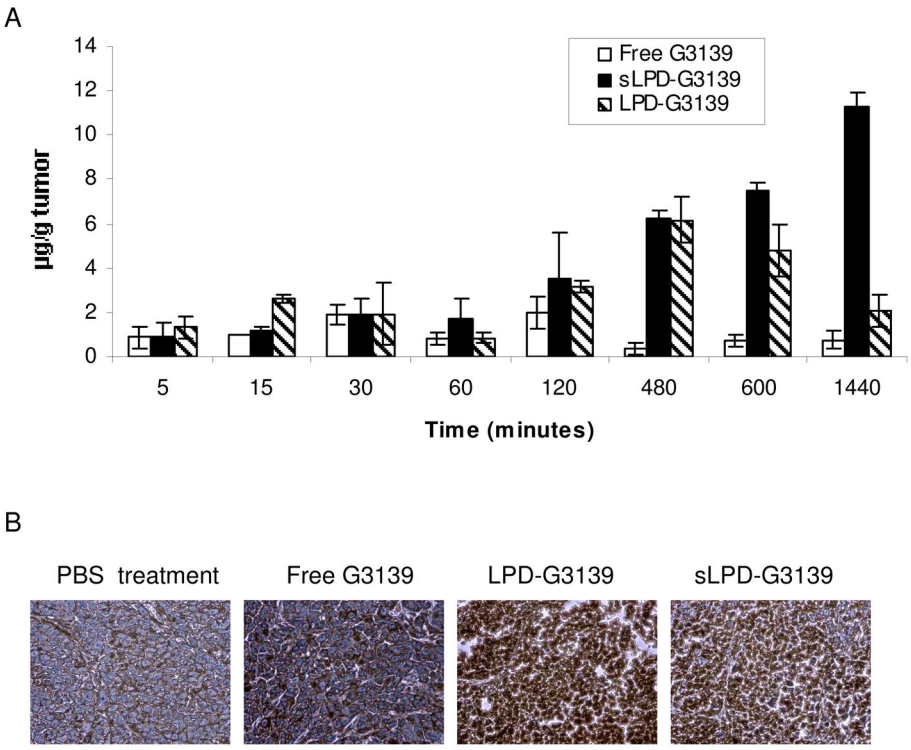

Figure 7.

G3139 accumulation and Bcl-2 expression in tumors

Panel A. Tumor accumulation profile of FAM-G3139. Following tail i.v. bolus administration of 5 mg/kg of FAM-G3139 loaded sLPD, LPD, or free FAM-G3139 in tumor-bearing mouse (n=3). Each point represents Mean ± SD of three mice.

Panel B. Immunohistochemical staining of Bcl-2 in tumors. Frozen sections were prepared from tumors after 4 times of 5 mg/kg treatment with free G3139 or sLPD-G3139 and stained with anti-human Bcl-2 antibodies.

NIH-PA Author Manuscript

NIH-PA Author Manuscript

NIH-PA Author Manuscript

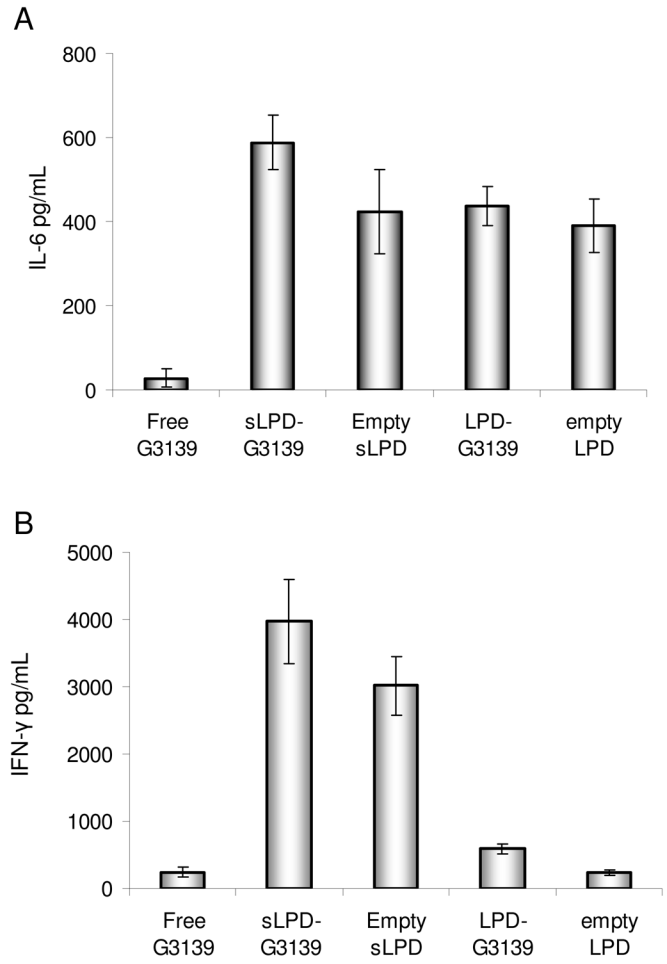

Figure 8.

Serum cytokine production in mice. After the treatment by sLPD-G3139 or controls (free G3139, LPD-G3139, empty sLPD or empty LPD), serum from the mice was collected and cytokine IL-6 and IFN-γ were detection by ELISA. The values in the plot represent the means of 3 separate experiments. Error bars were standard deviations, n=3.

Panel A. IL-6 measurement

Panel B. IFN-γ measurement.

NIH-PA Author Manuscript

NIH-PA Author Manuscript

NIH-PA Author Manuscript

Table 1

Effect of PEI-2k and Ca^{2+} on particle size of sLPD

Formulation	Size [a] (nm)
sLPDs	105.4±10.3
LPDs (without cis-11-hexadecenal)	108.8±7.3
sLPDs without PEI-2k	147.3±8.5[b]
sLPDs without Ca^{2+}	103.6±2.9

[a] Data represent the mean ± SD of three separate experiments (n=3).

[b] Data show significant difference compared to sLPD group ($p < 0.05$)

NIH-PA Author Manuscript
NIH-PA Author Manuscript
NIH-PA Author Manuscript

Table 2

Survival of mice after treatments by sLPD-G3139s

Formulation	Median survival time[a] (days)	T/C[a] (%)	Increase in lifespan[a] (%)	Log-rank *p* compared to PBS group[a]	Log-rank *p* compared to LPD-G3139 group[a]
PBS	28	100	0		
Free G3139	31[c]	110[c]	10[c]	0.425	
Empty LPD	32	114	14	0.378	
Empty sLPD	45[b]	161[b]	61[b]	0.022	
LPD-G3139	46[b]	164[b]	64[b]	0.017	
sLPD-G3139	56[bc]	200[bc]	100[bc]	0.009	0.012

[a] n=5 for each treatment group

[b] Data show significant difference compared to PBS control group

[c] Data show significant difference compared to LPD-G3139 group